



Potentials of Silicon Materials From Lake Chad and River Alau for Development of PV Panel

Tahiru Mohammed¹, M.B. Maina² and A.B. Muhammad³

¹²³Department of Mechanical Engineering University of Maiduguri, P.M.B. 1069 Borno State
Nigeria

Abstract: This study provides insights into the availability of local silicon resources, which can help sustain the growth of solar PV applications. It also explores the possibility of reducing dependency on external silicon sources by utilizing local sand, thereby enhancing economic feasibility and minimizing the environmental impact of transportation processes. The study utilized various analytical techniques such as X-Ray Fluorescence (XRF), X-Ray Diffraction (XRD), Potential of Hydrogen (pH), electrical conductivity (EC), Scanning Electron Microscopy (SEM), Energy Dispersive X-ray Spectroscopy (EDX), and MATLAB simulations to characterize the properties of the sand samples. The analysis revealed differences in silicon concentrations, oxide concentrations, physical properties (grain size distribution, porosity, density), and trace elements and impurities present in the sand samples. These factors have implications for panel efficiency, durability, and manufacturing processes. Based on the findings, River Alau's sand exhibited higher silicon content (86.16%) compared to Lake Chad's sand (69.62%). Simulations projected different efficiencies and performances of solar PV panels constructed using sands from both sources, with River Alau's sand showing more promise. However, Lake Chad's sand may require additional processing or blending with higher silicon sources to optimize panel manufacturing. The study's findings contribute to the understanding of local silicon availability and highlight potential strategies for the enrichment of sandstones for silicon production.

Keywords: Diffraction, X-Ray, Fluorescence, environmental impact and feasibility.

1.0 INTRODUCTION

Renewable energy sources such as solar energy, wind energy, biomass energy, ocean, and geothermal energy are currently prominent areas of research and energy generation. As of 2022, global energy production from renewables reached 3371 GW, with an increase of around 294 GW (Sah, et al., 2023). Solar energy in particular has garnered significant global attention, contributing more than half (approximately 191 GW) of the total renewable energy added in 2022 (Sah, et al., 2023). The cumulative installed capacity of solar photovoltaics (PV) globally has achieved a remarkable 1053 GW. A recent projection by the International Energy Agency (IEA) anticipates that solar photovoltaics will fulfil about 32% of the world's

total energy demand by 2050, necessitating the installation of 14 TW of PV capacity—more than three times the previous target of 4.5 TW (IEA, 2021a). However, the widespread adoption of solar PV systems may lead to an escalation in the demand for raw materials like silicon, posing a potential constraint on the sustainable growth of the PV industry.

The IEA (IEA, 2021) reports that the demand for silicon for PV solar in 2020 was about 390 thousand tonnes and this is projected to reach 452 thousand tonnes by the year 2030. The crystalline silicon PV system utilizes extremely pure silicon wafers to convert solar energy into electricity. The global market for crystalline silicon PV is propelled by a surging demand for renewable energy, a rise in electricity consumption driven by global population growth, and the imperative for efficient and economical renewable energy sources due to limited fossil fuel availability and stringent government regulations on carbon emissions. In comparison to alternative technologies like amorphous silicon and non-silicon solar cells, crystalline silicon solar cells exhibit high efficiency. However, obstacles such as the substantial initial investment and reduced efficiency of crystalline silicon under very high temperatures impede market growth. Anticipated growth opportunities in the market include technological advancements in solar cells to enhance efficiency and increased government investment in renewable energy projects.

Silicon ranks as the Earth's second most plentiful element in the crust. Currently, silicon has revolutionized various aspects of our daily existence due to its versatile applications, encompassing solar cells, energy storage, sensors, biological imaging, drug delivery, photonics, and electronic components. Silicon does not exist naturally in its free state but is typically found in combination with silica or silicates (Arunmetha, et al., 2018). Silicon is produced industrially by reduction of silicon dioxide with carbon in an electric arc furnace at temperatures higher than 2000 °C in the hottest parts, by a reaction that can be written ideally as (Boussaa, et al., 2017):



Silica is an inorganic material; it is the natural form of silicon dioxide (SiO_2), which is found in many minerals. Quartzite, silica sand and sandstone are all grouped together under one genetic name Silica minerals.

Sand results from the weathering processes that lead to the breakdown or decomposition of rocks near the Earth's surface. It is characterized as a clastic rock without any cement, featuring particle sizes ranging from 0.05 to 2 mm (Boussa, et al., 2016). While these grains can be composed of various minerals, the predominant constituent of sand is often quartz, a mineral composed of silica

(silicon dioxide). Ferromagnesian minerals refer to silicate minerals where iron and magnesium cations are essential components, encompassing minerals such as olivine, pyroxenes, amphiboles, and micas like biotite and phlogopite. To be suitable for industrial purposes, a specific source of sand must not only have a high silica content but must also adhere to strict limitations on metallic elements such as iron, aluminium, titanium, and others (Boussa, et al., 2016). This study intends to characterise and numerically analyse the potential solar PV application of silicon content of sand from River Alau and Lake Chad, Borno state, Nigeria.

2.0 MATERIALS AND METHOD

A diverse array of materials and equipment has been assembled to facilitate various experimental procedures and analyses. The following list outlines the essential tools, instruments and substances used to this investigation:

- i. Furnace
- ii. Filter paper
- iii. Conical flask
- iv. Amimia acetal
- v. Calcium chloride
- vi. Stirrer
- vii. Crucible
- viii. Digital balances
- ix. Conductivity meter
- x. Sample bag
- xi. Ph meter
- xii. SEM Machine
- xiii. XRD machine

2.1 Method

We randomly chipped soil samples from two main areas (Lake Chad and River Alau) that are devoid of agricultural land. The sample was brought to Ahmadu Bello University in Zaria's multi-user science lab so that the ensuing analysis could be done.

2.2. Physical and Chemical Properties Characterization of the Sample

2.2.1 X-Ray Fluorescence (XRF)

XRF is a non-destructive analytical technique used to determine the elemental composition of materials. XRF give details as to the chemical composition of a sample but will not indicate what phases are present in the sample. This XRF analysis serves as a fundamental step in understanding the chemical composition of the sand samples, laying the groundwork for subsequent analyses and considerations in assessing their potential utilization in solar PV panel manufacturing

XRF Analysis Procedure

1. A user fires an XRF gun at a sample.
2. Now stimulated by x-rays, the sample displaces inner-shell electrons, and outer-shell electrons take their place.
3. The XRF gun receives the fluorescent x-ray emissions, converts them to electrical pulses, and sends the pulses to an internal preamplifier.

2.2.2 Potential of Hydrogen (Ph) and Electrical Conductivity (EC)

Ph analysis is carried out in order to measure the acidity or basicity (alkalinity) of a soil and EC analysis is conducted to indicate the amount of soluble (salt) ions in soil. Plate 3.1 depicts the Ph tester used for Ph analysis.

Procedure for potential of hydrogen (ph) and electrical conductivity (EC)

A 10.0g sample of dry soil was be weighed and placed in either 50 or 100-ml beakers, with the addition of 25 ml of water to achieve a soil-to-water ratio of 1:2.5 w/v. The mixture was shaken, allowed to settle for 60 minutes, and then the water separated from the mixture. Subsequently, a pH/EC meter was inserted to obtain readings. To ensure accuracy, the process was repeated for obtaining precise results.

2.3 X-Ray Diffraction (XRD)

XRD is a technique used in materials science for determining the atomic and molecular structure of a material. XRD machine shown in Plate 2.1 is used in carrying out the analysis.

Procedure for XRD Analysis

The analyzed material was finely ground, homogenized, and average bulk composition is determined. The powdered sample was then prepared using the sample preparation block and compressed in the flat sample holder to create a flat, smooth surface that was later mounted on the sample stage in the XRD cabinet.

The sample was analysed using the reflection-transmission spinner stage using the Theta-Theta settings. Two-Theta starting position was 4 degrees and ends at 75 degrees with a two-theta step of 0.026261 at 8.67 seconds per step. Tube current was 40mA and the tension was 45VA. A Programmable Divergent Slit was used with a 5mm Width Mask and the Gonio Scan was used.

The intensity of diffracted X-rays is continuously recorded as the sample and detector rotate through their respective angles. A peak in intensity occurs when the mineral contains lattice planes with d-spacings appropriate to diffract X-rays at that value of θ . Although each peak consists of two separate reflections ($K\alpha_1$ and $K\alpha_2$), at small values of 2θ the peak locations overlap with $K\alpha_2$ appearing as a hump on the side of $K\alpha_1$. Greater separation occurs at higher values of θ . Typically these combined peaks are treated as one. The 2λ position of the diffraction peak is typically measured as the centre of the peak at 80% peak height.

Results are commonly presented as peak positions at 2θ and X-ray counts (intensity) in the form of a table or an x-y plot (shown above). Intensity (I) is either reported as peak height intensity, that intensity above background, or as integrated intensity, the area under the peak. The relative intensity (RI) is recorded as the ratio of the peak intensity to that of the most intense peak i.e.,

$$RI = \frac{I}{I_x} \times 100 \quad (3.1)$$



Plate 2.1: XRD machine

2.2.3 Scanning Electron Microscopy (SEM)

SEM is a test process that scans a sample with an electron beam to produce a magnified image for analysis. The method is also known as SEM analysis and SEM microscopy, and is used very effectively in microanalysis and failure analysis of solid inorganic materials. Plate 2.2 presents the SEM Machines Setup

SEM analysis procedures

1. Step 1: Specify the model. In the model specification, the researcher specifies the model by determining every relationship between variables relevant to the researcher's interest.
2. Step 2: Identify the model
3. Step 3: Estimate the model.
4. Step 4: Test the model fit.
5. Step 5: Manipulate the model.



Plate 2.2: SEM Machines Setup

2.2.4 Energy Dispersive X-Ray Analysis (EDX)

EDX also referred to as EDS or EDAX, is an X-Ray technique used to identify the elemental composition of materials. Applications include materials and product research, troubleshooting, de-formulation, and more. XRD can determine the presence and amounts of minerals species in sample, as well as identify phases.

Procedure for EDX

X-rays are generated using EDX following a two-step process.

First, the energy transferred to the atomic electron knocks it off, leaving behind a hole. Second, its position is filled by another electron from a higher energy shell, and the characteristic X-ray is released.

2.3 Simulation and Analysis

MATLAB was employed in the analysis and the test was performed based on the PV panel capacity of 150 W.

2.3.1 Output Power

In general, the power output of a device is the product of the voltage and current on that product. For V and I respectively denoting voltage in Volts and current in Amperes, the power generated by a device with resistance R in ohms is:

$$P = VI = I^2R = \frac{V^2}{R} \quad (3.2)$$

In particular for a solar module,

$$P = V_{mp} I_{mp} \quad (3.3)$$

V_{mp} and I_{mp} correspond to the maximum voltage and current at maximum power P_{max} . These voltage and current values can be determined empirically when rating a module. Hence, the pair (V_{mp}, I_{mp}) can be obtained from the device simultaneously.

2.3.2 Panel Efficiency

The efficiency (η) of the module is the ratio of output power to input power:

$$\eta = \frac{P_{max}}{P_{in}} \quad (3.4)$$

2.3.3 Simulation Execution

The simulation was run by using the developed model (developed program) and incorporating the EDX-derived silicon atomic concentration data.

2.3.4 Analysis of Result

The power output was simulated and evaluated under varying conditions (light intensity, temperature and irradiance) and analyses how changes in silicon atomic concentration affect performance.

3.0 RESULTS AND DISCUSSION

3.1 Characterization of Results

The X-Ray Fluorescence (XRF) analysis results are presented in Figures 4.1 and 4.2. The Figures provide a detailed overview of the oxide concentrations within the sand samples obtained from River Alau and Lake Chad. The unit percentages of various oxides are crucial

indicators of the chemical composition of the samples, shedding light on their suitability for solar photovoltaic (PV) panel formation.

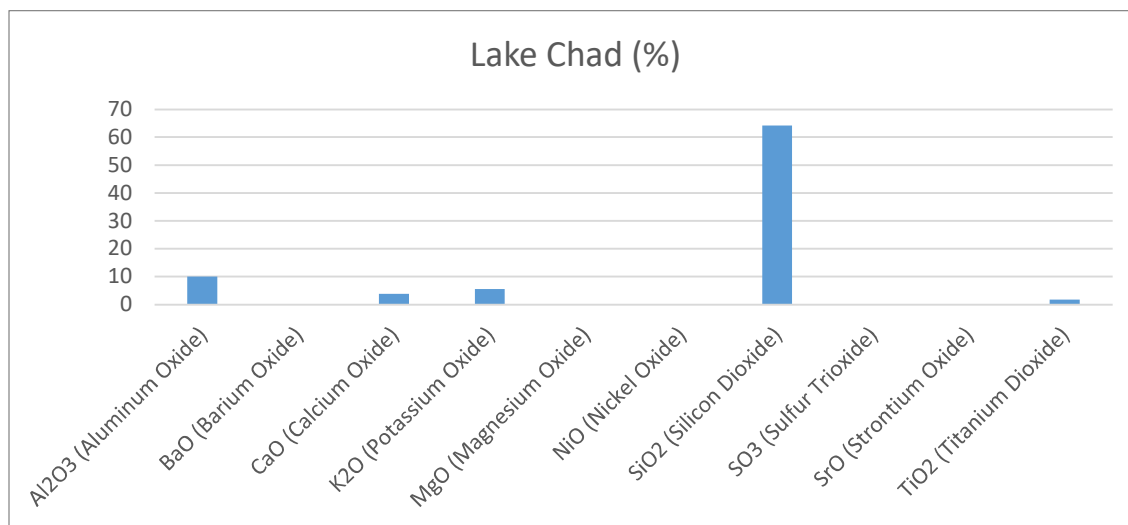


Figure 3.1: Lake Chad Sand XRF analysis

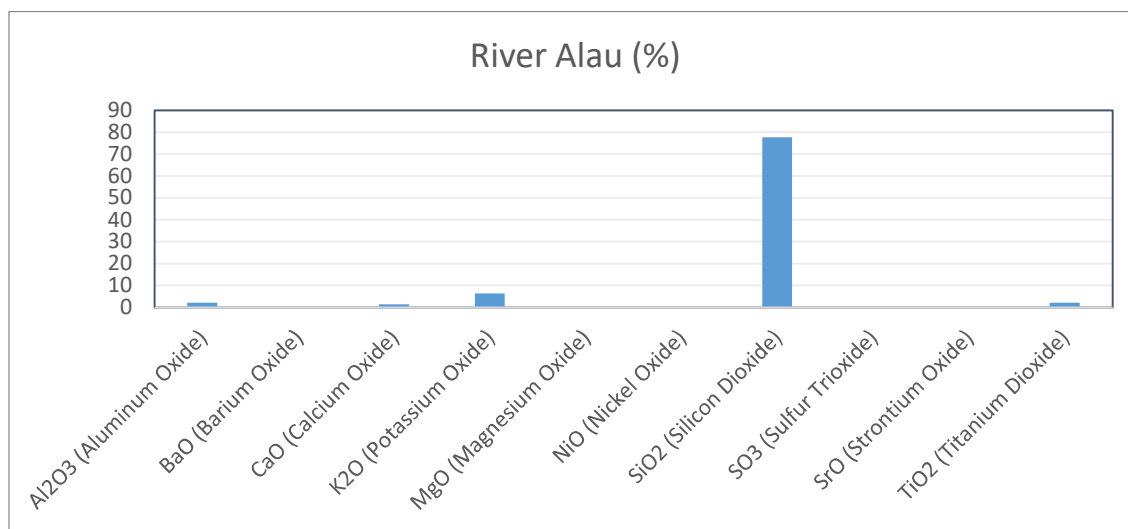


Figure 3. 2: River Alau Sand XRF analysis

3.2 pH and Electrical Conductivity Measurements

The Table 3.1 presents the pH and electrical conductivity (EC) measurements of sands from River Alau and Lake Chad. These parameters provide crucial insights into the chemical nature and suitability of the sand for specific applications, including their potential use in solar photovoltaic (PV) panel production.

The pH measurement for River Alau sand is recorded at 6.68, indicating a slightly acidic nature. A pH value close to 7 suggests a neutral to slightly acidic environment. This pH level

might influence the sand's chemical reactions and interactions during processing stages for solar panel fabrication. In contrast, the pH measurement for Lake Chad sand is higher, recorded at 7.25. This value leans more towards neutrality. A pH closer to neutral might imply fewer acidic or basic reactions during the sand's processing for solar panel manufacturing. The pH levels of the sand samples might influence chemical reactions during the production of solar panels. While both samples are relatively close to neutral, the slight differences could impact reactions involving chemicals used in the panel manufacturing process. However, these pH values are within ranges that are generally manageable in industrial processes.

The electrical conductivity of River Alau sand stands at 8.51 $\mu\text{S}/\text{cm}$, indicating a relatively low conductivity level. Low electrical conductivity can suggest a lower concentration of dissolved ions in the sand, which could impact its behavior during certain industrial processes. In contrast, the EC measurement for Lake Chad sand is substantially higher at 90.60 $\mu\text{S}/\text{cm}$. This markedly elevated electrical conductivity suggests a higher concentration of dissolved ions or salts in the sand. Higher conductivity might influence the sand's behavior in various manufacturing processes.

The pH and electrical conductivity measurements provide initial insights into the chemical nature and potential reactivity of the sand samples sourced from River Alau and Lake Chad. While both samples exhibited relatively neutral pH levels, the considerable difference in electrical conductivity suggests variations in dissolved ion concentrations that could impact industrial processes involving these sands. Further investigations are necessary to precisely identify the specific ions or salts present and their concentrations, as well as to understand how these factors might affect the sand's behavior during solar panel manufacturing processes. This analysis lays the groundwork for more detailed studies to assess the overall suitability of these sands for use in solar PV panel production.

Table 3.1: Potential of hydrogen (ph) and Electrical Conductivity (EC) results

S/No.	Sample	PH	Conductivity ($\mu\text{S}/\text{CM}$)
1	River Alau Sand	6.68	8.51
2	Lake Chad Sand	7.25	90.60

3.3 SEM and EDX Analysis Results Silicon Content Analysis

The SEM and EDX analyses revealed the atomic and weight concentrations of silicon in the sand samples. The analysis depicted that the silicon content in Lake Chad sand was detected at an atomic concentration of 69.62% and a weight concentration of 65.59%. Despite containing substantial silicon content, these measurements fall below the standard required for making PV cells efficiently. In comparison, the silicon content in River Alau sand exhibited higher concentrations, with an atomic concentration of 86.16% and a weight concentration of 85.43%. While this sample

demonstrates significantly higher silicon content compared to Lake Chad, it still falls short of meeting the standard necessary for PV cell production. The SEM and EDX analyses underscore the significance of silicon content in the sands from River Alau and Lake Chad. Despite showing notable silicon concentrations, both samples fall below the industry-standard threshold required for efficient PV cell manufacturing.

3.4 Simulation Analysis Using MATLAB

The simulations provided insights into the potential challenges and advantages of using these sands for solar panel formation, allowing for informed decision-making in panel manufacturing. Figures 4.3 and 4.4 show the power output as function of silicon concentration. The horizontal axis (X-axis) represents the silicon concentration and the vertical axis (Y-axis) represents the power output, measured in Watts. This is the amount of power generated by the system associated with the samples. The Figures show for a given solar irradiance; the power output increases with increase in silicon concentration. This pattern is noticed for both the river Alau sand and the Lake Chad sand. The underlying reason for this pattern is attributed to the semiconductor properties of silicon. As the concentration of silicon in the samples rises, it enhances the material's ability to efficiently convert solar energy into electrical power. Silicon, a key component in solar cells, plays a crucial role in absorbing sunlight and facilitating the generation of electric current. Therefore, the positive correlation between silicon concentration and power output suggests that higher silicon levels contribute to improved energy conversion efficiency in the studied samples. This finding underscores the significance of silicon concentration in influencing the overall performance of the power generation system under various solar irradiance conditions.

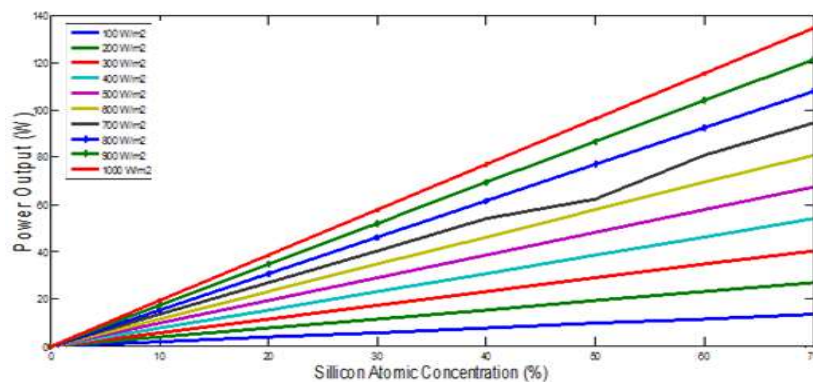


Figure 3.3: Lake Chad Power Output (W)

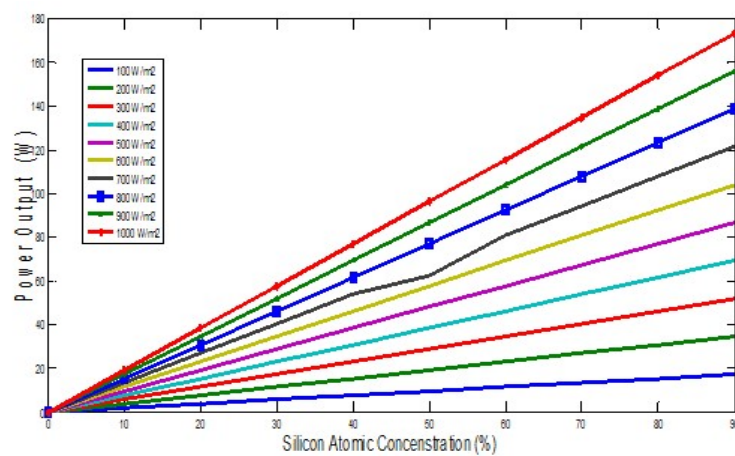


Figure 3.4: River Alau Power Output

4.0 Conclusion

Silicon Content Assessment for the two sample areas has been achieved where the silicon content analysis revealed varying concentrations in the sand samples from River Alau and Lake Chad. River Alau's sand (86.16%) showed higher silicon content compared to Lake Chad's (69.62%) samples.

Physical and Chemical Properties: The physical properties such as grain size distribution, porosity, and density were measured, showing differences between the samples. Chemical analyses identified trace elements and impurities, affecting the suitability for solar panel formation were also determined.

Simulation Results: The findings were simulated to project the potential efficiency and performance of solar PV panels constructed using the sands from both sources. Simulations indicated variations in panel performance due to differing silicon content and impurities as duly captured in the findings.

This study highlights the significance of silicon content in sand for solar PV panel development. It was found that River Alau's sand shows a promising future due to its higher silicon content, while Lake Chad's sand might require additional processing or blending with higher silicon sources for optimal panel manufacturing. The physical and chemical properties, along with simulation results, collectively indicate the complexities and considerations involved in utilizing sand for solar panel development which shows that aim and objectives of the study has been achieved.

REFERENCES

- Ahlers, C. (2018). *Silicon from sand*. Retrieved November 30, 2023, from <http://blog.teachersource.com/2011/03/02/silicon-from-sand/>
- Alkan, G., Mechnich, P., & Pernpeintner, J. (2022). Improved Performance of Ceramic Solar Absorber Particles Coated with Black Oxide Pigment Deposited by Resonant Acoustic Mixing and Reaction Sintering. *Coatings*, 12, 757.
- Arunmetha, S., Vinoth, M., Srither, S. R., Karthik, A., Sridharpanday, M., Suriyaprabha, R., . . . Rajendran, V. (2018). Study on production of silicon nanoparticles from quartz sand for hybrid solar cell applications. *Journal of Electronic Materials*, 47(1), 493-502.
- Boussa, S. A., Kheloufi, A., Zaourar, N. B., & Kerkar, F. (2016). Valorization of Algerian sand for photovoltaic application. *Acta Physica Polonica A*, 130, 133-137.
- Boussaa, S. A., Kheloufi, A., Zaoirar, N. B., Kefai, A., & Kerkar, F. (2017). Characterization of silica sandstone for photovoltaic application. *Journal of Materials, Processes and Environment*, 5(1), 76-79.
- Chang, W.-S., Park, C.-M., Kim, J.-H., Kim, Y.-U., Jeong, G., & Sohn, H.-J. (2012). Quartz (SiO₂): a new energy storage anode material for Li-ion batteries. *Energy & Environmental Science*, 5(5), 6895.

- Chung, K. M., & Chen, R. (2023). Black coating of quartz sand towards low-cost solar-absorbing and thermal energy storage material for concentrating solar power. *Solar Energy*, 249, 98-106.
- De La Rocha, C. (2022). *From Sand to Solar Modules: The Construction of Solar Cells*. Retrieved November 29, 2023, from <https://www.unsustainablemagazine.com/from-sand-to-solar-modules/>
- Farirai, F. O., Aniokete, T. C., Eterigho-Ikelegbe, O., Mupa, M., Zeyi, B., & Daramola, M. O. (2020). Methods of extracting silica and silicon from agricultural waste ashes and application of the produced silicon in solar cells: a mini-review. *International Journal of Sustainable Engineering*, 1-22.
- Flogeac, K., Guillon, E., Aplincourt, M., Marceau, E., Stievano, L., Beaunier, P., & Frapart, Y. (2005). Characterization of soil particles by X-ray diffraction (XRD), X-ray photoelectron spectroscopy (XPS), electron paramagnetic resonance (EPR) and transmission electron microscopy (TEM). *Agronomy for Sustainable Development*, 25(3), 345-353.
- Furquan, M., Raj Khatriail, A., Vijayalakshmi, S., & Mitra, S. (2018). Efficient conversion of sand to nano-silicon and its energetic Si-C composite anode design for high volumetric capacity lithium-ion battery. *Journal of Power Sources*, 382, 56-68.
- Gimeno-Furio, A. H., Martinez-Cuenca, R., Mondragón, R., Vela, A., & Cabedo, L. (2020). New coloured coatings to enhance silica sand absorbance for direct particle solar receiver applications. *Renewable Energy*, 152, 1-8.
- Gimeno-Furio, A. H., Martinez-Cuenca, R., Mondragón, R., Vela, A., Cabedo, L., & Iacob, M. (2020). New coloured coatings to enhance silica sand absorbance for direct particle solar receiver applications. *Renewable Energy*, 152, 1-8.
- Hamed, H., Hale, W., & Stern, B. (2021). X-ray diffraction to determine the mineralogy in soil samples in the UK. *International Journal of Engineering Applied Sciences and Technology*, 5(10), 91-98.
- Heidari, S. M., & Anctil, A. (2022). Country-specific carbon footprint and cumulative energy demand of metallurgical grade silicon production for silicon photovoltaics. *resources, conservation and Recycling*, 180, 106171.
- Ho, C. K. (2016). A review of high-temperature particle receivers for concentrating solar power. *Applied Thermal Engineering*, 109, 958-969.
- Humood, M., Beheshti, A., Meyer, J. L., & Polycarpou, A. A. (2016). Normal impact of sand particles with solar panel glass surfaces. *Tribology International*, 102, 237-248.
- IEA. (2021). *Demand for silicon from solar PV by scenario 2020-2040*. Retrieved November 28, 2023, from <https://www.iea.org/data-and-statistics/charts/demand-for-silicon-from-solar-pv-by-scenario-2020-2040>
- IEA. (2021a). *Net Zero by 2050*. Paris: IEA. Retrieved from <https://www.iea.org/reports/net-zero-by-2050>

- IEA. (2021b). *Demand for silicon from solar PV by scenario 2020-2040*. Retrieved November 28, 2023, from <https://www.iea.org/data-and-statistics/charts/demand-for-silicon-from-solar-pv-by-scenario-2020-2040>
- Islam, M. R., Kuddus, A., Akter, A., Hossain, S., & Ismail, A. B. (2019). Application of Si-NPs Extracted from the Padma River Sand of Rajshahi in Photovoltaic Cells. *2019 International Conference on Computer, Communication, Chemical, Materials*.
- Kasavajjula, U., Wang, C., & Appleby, A. J. (2007). Nano- and bulk-silicon-based insertion anodes for lithium-ion secondary cells. *Journal of Power Sources*, 163(2), 1003–1039.
- Kim, T. K., VanSaders, B., Caldwell, E., Shin, S., Liu, Z., Jin, S., & Chen, R. (2016). Copper-alloyed spinel black oxides and tandem-structured solar absorbing layers for high-temperature concentrating solar power systems. *Solar Energy*, 132, 257–266.
- Maldonado, S. (2020). The Importance of New “Sand-to-Silicon” Processes for the Rapid Future Increase of Photovoltaics. *ACS Energy Letters*, 5(11), 3628-2632.
- Muller, J.-C., & Siffert, P. (2004). Silicon for Photovoltaics. *Silicon*, 2, 73–79.
- Palacios, A., Barreneche, C., Navarro, M. E., & Ding, Y. (2019). Thermal energy storage technologies for concentrated solar power – A review from a materials perspective. *Renewable Energy*.
- Quercia, G., van der Putten, J. J., Hüsken, G., & Brouwers, H. J. (2013). Photovoltaic’s silica-rich waste sludge as supplementary cementitious material (SCM). *Cement and Concrete Research*, 54, 161–179.
- Sah, D., Chitra, U. N., Saravanan, M., & Kumar, S. (2023). Growth and analysis of polycrystalline silicon ingots using recycled silicon from waste solar module. *Solar Energy Materials and Solar Cells*, 261, 112524.
- Sdiri, A., Higashi, T., Bouaziz, S., & Benzina, M. (2014). Synthesis and characterization of silica gel from siliceous sands of southern Tunisia. *Arabian Journal of Chemistry*, 7(4), 486–493.
- Shimpo, S., Tu, H. T., & Ohdaira, K. (2023). Potential-induced degradation of encapsulant-less p-type crystalline Si photovoltaic modules. *Japanese Journal of Applied Physics*, 62, SK1039.
- Skoczek, A., Sample, T., & Dunlop, E. D. (2009). The results of performance measurements of field-aged crystalline silicon photovoltaic modules. *Progress in Photovoltaics: Research and Applications*, 17(4), 227–240.